JOURNAL OF ELECTROMAGNETIC ENGINEERING AND SCIENCE, VOL. 13, NO. 4, 251－258, DEC. 2013

http://dx.doi.org/10.5515/JKIEES.2013.13.4.251
ISSN 2234-8395 (Online) · ISSN 2234-8409 (Print)

Parameter Selection Procedure of Parabolic Reflector Antenna for the Optimum Synthetic Aperture Radar Performances

Seong Sik Yoon[1] · Jae Wook Lee[1,*] · Taek Kyung Lee[1] · Dong Woo Yi[2]

Abstract

A procedure for antenna parameter selections is proposed that considers the relationships between synthetic aperture radar performance and the antenna parameters of a parabola-type reflector antenna with a central flat dish. The effects of a central dish designed for weight reduction on the antenna beam pattern are also quantitatively analyzed using commercially available software based on the physical optics algorithm. The results of the theoretical analysis and simulation predict that a larger size of the central dish results in an increase in the sidelobe level, which is the reason for the increase in two important ambiguities, such as range ambiguity ratio (RAR) and azimuth ambiguity ratio (AAR). The dependence of RAR and AAR on Pulse repetition frequency is also analyzed and discussed.

Key Words: Azimuth Ambiguity, Backscattering Coefficient, Central Dish, PRF, Range Ambiguity, Reflector Antenna, Sidelobe Level.

Ⅰ. Introduction

In general, the images captured from real aperture radar systems can be acquired through the rearrangement of one-dimensional (1D) radar signals obtained by the motion of the radar platform into 2D radar signals [1]. However, the image resolution in the azimuth direction is directly dependent on both the distance from the radar platform to target and the radiated beamwidth, so a narrower beamwidth has been required for the radiation pattern in the radar system as the altitude of the operating radar system increases. In addition, higher resolution at the mm-level in a radar system operating at higher altitudes, such as a satellite, requires that the antenna mounted on the radar platform have a physical size that is too big and impractical to be realized.

The resolution in the azimuthal direction in synthetic aperture radar (SAR) systems could be improved by rearranging the detected 2D signals and carrying out signal-processing in the azimuthal direction. The SAR system can operate under all weather conditions and covers a wide area with high resolution. Therefore, its use can lead to a size reduction in the overall radar system, which is an increasing trend in public needs, science, and military demands.

Many researchers have studied and investigated aspects of quality improvement in the detected signals and images [2, 3]. The ambiguity level specified by the SAR performance evaluations is a particularly important parameter for testing the error rate that frequently occurs in the signal reception. Mistakes in image information due to potential ambiguity of the detected signal have been mentioned in [4, 5].

Previous studies aimed at resolving this ambiguity problem have been conducted almost exclusively in the signal processing stage. However, if the ambiguity could be alle-

Manuscript received November 15, 2013 ; Revised December 2, 2013 ; Accepted December 5, 2013. (ID No. 20131115-048J)
[1]Department of Electronics, Telecommunication and Computer Engineering, Korea Aerospace University, Goyang, Korea.
[2]Agency for Defense Development, Daejeon, Korea.
[*]Corresponding Author: Jae Wook Lee (e-mail: jwlee1@kau.ac.kr)

viated by a properly designed antenna, a significant reduction would be expected in the system complexity and processing difficulties. In this paper, we suggest parameter selection procedures for determining the antenna and electrical performance of an overall radar system that would reduce the ambiguity and improve image resolution as key parameters of SAR performance.

Section Ⅱ presents the structure and beam pattern analysis for the given geometry of reflector antenna for the SAR system. The parameter values affecting SAR performance are also derived, with the inclusion of backscattering coefficients into the ambiguity calculations, which leads to an increased reliability. In Section Ⅳ, the optimized antenna parameter values have been determined through parametric studies on the relationship between SAR performance and antenna parameters. Finally, conclusions are briefly described, together with the analysis results.

Ⅱ. Reflector Antenna for SAR

In general, a satellite SAR antenna requires high gain and narrow beamwidth for high resolution of the detected image with pulsed transmitting/receiving transmission. Three well-known candidates satisfy the requirements for SAR performance: the conventional waveguide, a patch using an organic substrate, and a reflector antenna with a metallic solid surface. For instance, a waveguide slot array antenna has been employed for TerraSAR-X, the representative German satellite system [6]. Another example is the phased array antenna with a patch-type organic substrate used on the Canadian Radarsat-2 satellite, and the Italian Cosmo-SkyMed satellite [7, 8]. Reflector-type antennas have a drawback in their packaging efficiency relative to the waveguide or path array antenna, but they have advantages of high gain, narrow beamwidth, and easy implementation with transmit/receiving modules because of the possibility of a deployable mechanism [9].

This paper introduces a solid metal type of reflector antenna as a possible candidate for the SAR antenna system. In particular, the use of a flat dish with a given solid type of reflector antenna makes the antenna easy to manufacture and light weight, with low development costs. For instance, the center of the reflector antenna adopted in TecSAR system has been implemented with a flat surface [9].

Fig. 1 shows the ray tracing and moving path of the signal radiated from the feeding part, simulated and illustrated with a conventional and a modified reflector antenna structure. The electrical performance of these structures is analyzed using GRASP of TICRA, based on physical optics (PO). The dotted lines in Fig. 1 represent the equi-phase plane of the reflected rays from the reflectors. At this time, a Gaussian beam pattern is considered as an input signal generated from conical horn antenna as a feeding structure.

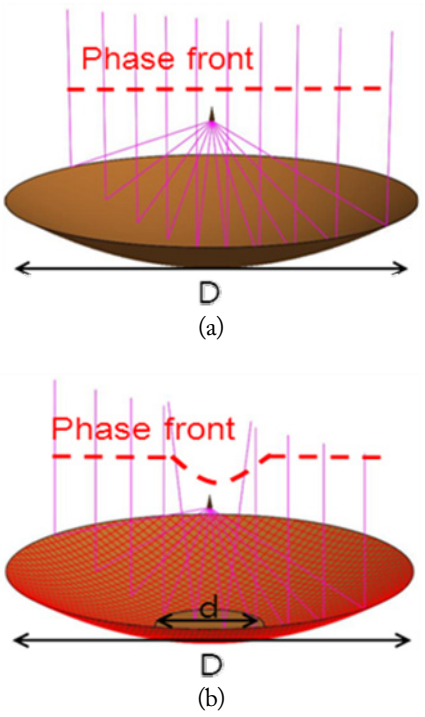

Fig. 1. Ray distributions in a conventional parabolic reflector antenna (a) and the proposed antenna with modification (flat surface) in its central part (b).

$$E_a(\rho) = F_f\left(\theta_f = 2\tan^{-1}\frac{\rho}{2F}\right)\frac{1}{1+\left(\frac{\rho}{2F}\right)^2}$$

$$= 20\log\left|F_f\right| - 20\log\left[1+\left(\frac{\rho}{2F}\right)^2\right](dB) \quad (1)$$

$$EI\,(\text{Edge Illumination}) = 20\log\left[E_a(\rho)\right] \quad (2)$$

Eqs. (1) and (2) represent the normalized electric field at the aperture and edge illumination, respectively, where F_f is the normalized radiation pattern in the feeding antenna, and ρ and F denote the axis of the aperture and focal distance, respectively [10].

Fig. 2 shows that the edge illumination affects the radiation pattern and directivity of reflector antenna and determines the trade-off between the aperture taper efficiency and spill-over efficiency.

The conventional parabolic reflector antenna, as expected from Fig. 1(a), has all the rays reflected from the reflector propagating to the aperture plane with equal distance; consequently, the detected electric fields will have uniform phase distributions. On the other hand, Fig. 1(b) shows that the reflected signals from the flat surface do not propagate in parallel with each other and finally distort the wave propagating in other directions, leading to non-uniform phase distributions at the aperture plane.

Next, we will investigate the magnitude distribution of

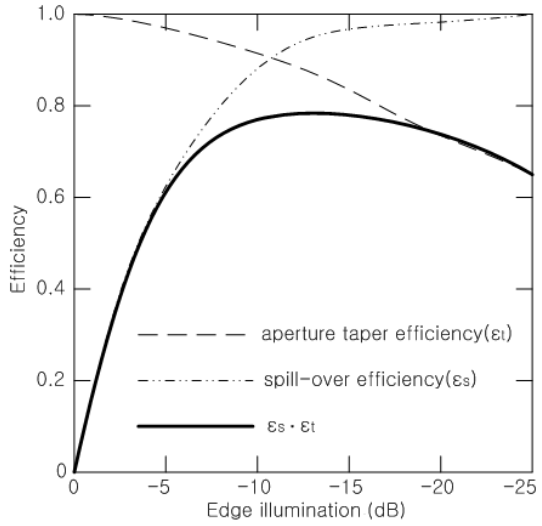

Fig. 2. The efficiency of reflector antenna according to the edge illumination.

electric fields at the aperture plane. Fig. 3 shows the normalized electric field distribution at the aperture plane.

The magnitude of all the electric field distributions, according to the positions at the aperture plane, has been normalized to the maximum electric field intensity at the looking angle of feed horn, which means the direction of the shortest path.

It is conjectured from Fig. 3 that the field distribution of the parabolic reflector antenna of Fig. 1(a) forms a parabolic tapered shape because of the spherical radiation beam from the feeding part and the falling-off characteristic, which is inversely proportional to the distance squared.

In contrast, in Fig. 1(b), the reflected wave from the flat surface at the center superposes on the other waves reflected from the other surfaces in a parabolic shape with different phase and magnitude.

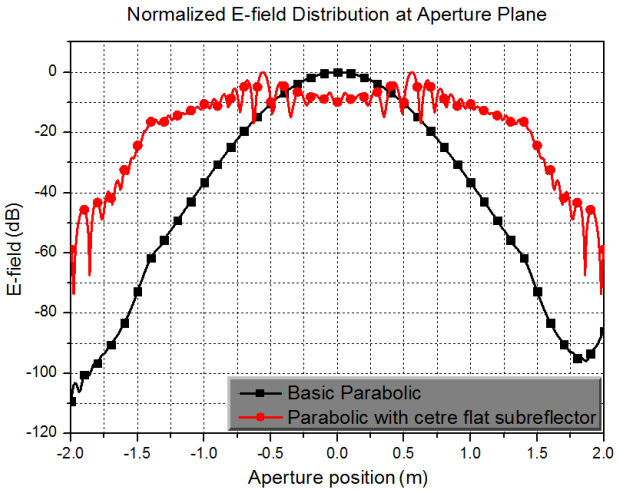

Fig. 3. Normalized electric field distributions for two types of antennas.

Table 1. Antenna characteristics according to the circular aperture taper

n	HPBW (rad)	Sidelobe level (dB)
0	$1.02\frac{\lambda}{D}$	−17.6
1	$1.27\frac{\lambda}{D}$	−24.6
2	$1.47\frac{\lambda}{D}$	−30.6

HPBW = half power beamwidth.

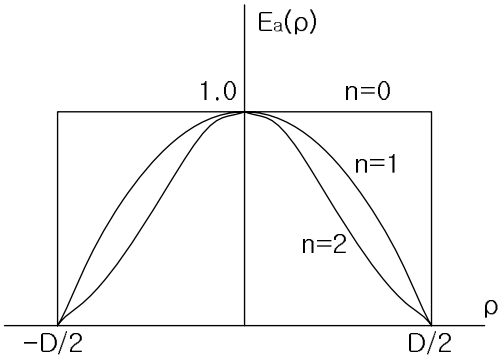

Fig. 4. Aperture field distribution at the circular aperture.

As a result, the field distribution at the superposed region corresponding to $\pm 0.2 \leq \rho \leq \pm 0.75$ shows only slight fluctuation as well as a relatively uniform distribution due to the summation of many other waves reflected from the surface.

$$E_a(\rho) = \left[1 - \left(\frac{2\rho}{D}\right)^2\right]^n \tag{3}$$

$$f(\theta) = \int_0^{2\pi}\int_0^{D/2} E_a(\rho) e^{j\beta\rho\sin\theta\cos(\phi-\phi')}\rho\, d\rho\, d\phi \tag{4}$$

Table 1 describes the half power beamwidth and sidelobe level according to the aperture field distributions given in Fig. 4 [10]. The results of Table 1 and Fig. 4 predict that the normalized field distributions of the reflector antenna with a flat subreflector shown in Fig. 3 will give a narrow beamwidth and higher sidelobe level. The theoretical approach has been verified by simulating the radiation patterns and investigating them using the commercially available and PO-oriented software GRASP of TICRA.

Fig. 5 shows the radiation pattern according to the radii of the flat surface in the proposed reflector antenna. As the radius becomes longer, the sidelobe level increases and the mainlobe gain is reduced.

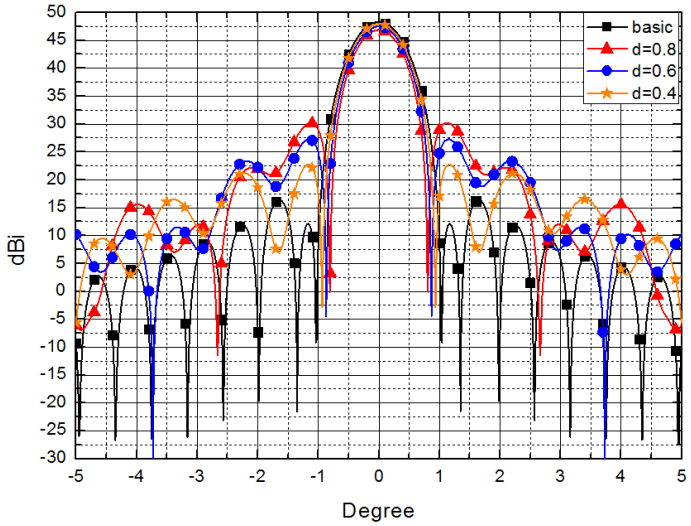

Fig. 5. The radiation pattern according to the radii of a flat surface.

Ⅲ. SAR Performance Evaluation

This section describes two ambiguity ratios as a function of sidelobe level effects.

1. The Range Ambiguity Ratio

The range ambiguity is thought to be a signal contamination due to the antenna sidelobe and the range difference between the desired and the ambiguity signal. Fig. 6 shows the operating concept of the SAR system with data acquisition geometry in a strip-map mode. Each parameter related to range ambiguity and azimuth ambiguity is included in Fig. 6. In general, the range ambiguity condition and its corresponding look angle can be calculated, respectively, using the following equations [1],

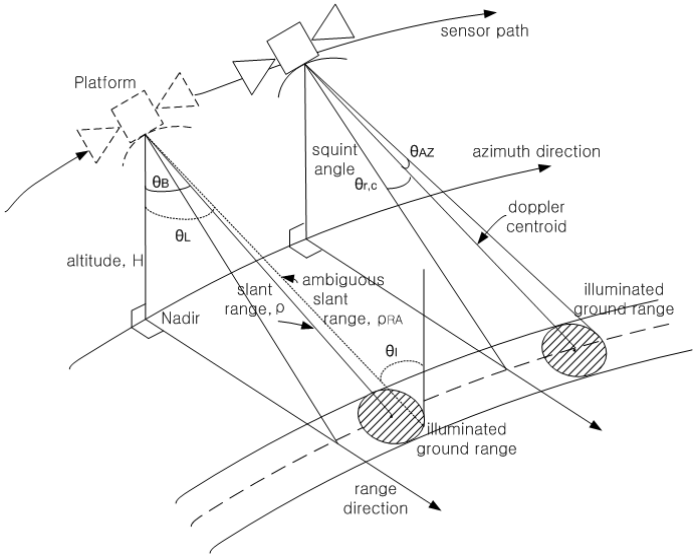

Fig. 6. The general concept of the synthetic aperture radar system.

$$\rho_{RA}(n) = \rho + \frac{n}{2}\frac{c}{PRF} \tag{5}$$

$$\cos\left(\theta_L(n)\right) = \frac{H^2 + \rho^2{}_{RA}(n) + 2RH}{2\rho_{RA}(n)(R+H)} \tag{6}$$

where $\rho_{RA}(n)$ is the range ambiguity slant range, H is the platform altitude, and R is the Earth radius. By newly defining the antenna angle, θ_A as

$$\theta_A(n) = \theta_L(n) - \theta_B, \tag{7}$$

the range ambiguity ratio (RAR) can be written as follows,

$$RAR = \frac{\sum_{n\neq 0} \dfrac{G_t(\theta_A(n))G_r(\theta_A(n))\sigma(\theta_A(n))}{\rho_{RA}{}^3(n)\sin(\theta_I(n))}}{\dfrac{G_t(\theta_A(0))G_r(\theta_A(0))\sigma(\theta_A(0))}{\rho^3\sin(\theta_I)}} \tag{8}$$

where G_t and G_r are gains of the transmitter and receiver antennas, respectively, and σ is the backscattering cross section depending on the incidence angle, θ_I.

2. The Azimuth Ambiguity Ratio

Azimuth ambiguity contamination is often generated by the aliased signals of Doppler information, as indicated by Eqs. (9) and (10) [1].

$$f_D = \frac{2V\sin(\theta_{AZ})}{\lambda} \tag{9}$$

$$f_D + n\,PRF = \frac{2V\sin(\theta_{AZ}(n))}{\lambda} \tag{10}$$

The V and θ_{AZ} refer to the velocity of the platform and the azimuth angle in the direction of the moving system, respectively. The azimuthal beam direction $\theta_{AZ}(n)$ is determined from the integral multiple, n of the Pulse repetition frequency (PRF) in the Doppler centroid. From the obtained angle generating the azimuth ambiguities, azimuth ambiguity ratio (AAR) can be written as follows [1]:

$$AAR = \frac{\sum_{n\neq 0}\int_{PB} G_t(\theta_{AZ}(n))G_r(\theta_{AZ}(n))\sigma(\theta_{AZ}(n))d\theta_{AZ}(n)}{\int_{PB} G_t(\theta_{AZ}(0))G_r(\theta_{AZ}(0))\sigma(\theta_{AZ}(0))d\theta_{AZ}(0)} \tag{11}$$

where PB means the Doppler processing bandwidth.

Ⅳ. Analysis Results

In this section, the relationship between SAR performance and antenna parameters is analyzed using the simulation results for the reflector antenna with the flat dish at the central part and applying the theoretical approach of SAR performance. Table 2 describes several parameters and values for the performance investigation of the SAR system.

Table 2. Parameters and values for SAR performance analysis

Parameter	Value or range
Carrier frequency (GHz)	9.6
Reflector size, $D \times D$ (m)	3×3
Altitude, H (km)	500
Platform velocity (km/s)	7.6
Squint angle (°)	20
SAR mode	Strip map
Flat dish size, d (m)	0.4−0.8 (interval, 0.1)
PRF (kHz)	7−12 (interval, 1)
Pulse incidence angle (°)	15−50 (interval, 5)
Polarization	VV

SAR = synthetic aperture radar, PRF = Pulse repetition frequency.

1. Backscattering Coefficients

The backscattering coefficient is an important parameter for radar performance, and should be taken into account when considering the surface reflection characteristics coming back from the target. In addition, the backscattering coefficient, σ is also dependent on the incidence beam angle and works as a multiplication factor with antenna gain. According to [11], the derived backscattering coefficient, as a function of the surface reflection characteristic and look angle, can be represented by using the surface reflectivity model [12]:

$$\sigma(\theta_L) = k_1 \exp\left(-\tan^2 \theta_L / a^2\right) + k_2 \exp\left(-\tan^2 \theta_L / b^2\right) \quad (12)$$

Where k_1 and k_2 represent the coefficients determined by the reflection characteristics of the target surfaces. The other parameters, a and b, are the standard deviations caused by the surface roughness, which were obtained from the least square approximation of numerous experimental data.

2. SAR Performance Analysis

Investigation of the ambiguity signal level according to the electrical performance of the antenna requires determination of the angle, θ_A which affects the signal contamination relative to the desired signal in the range direction.

Fig. 7 shows the RAR-generating angle in the range direction with the 2D antenna beam pattern according to variations in PRF. The look angle is assumed to be 30°. As predicted from Eq. (5), the slant range changes uniformly while the ambiguity-generating angle occurs at the beam illuminating angle ($\theta_A = 0°$) nearest to the positive integer, n. In addition, as the PRF increases, the range ambiguity signal also increases in the angle nearest to the mainlobe.

Figs. 8 and 9 show the graphs of RAR values according

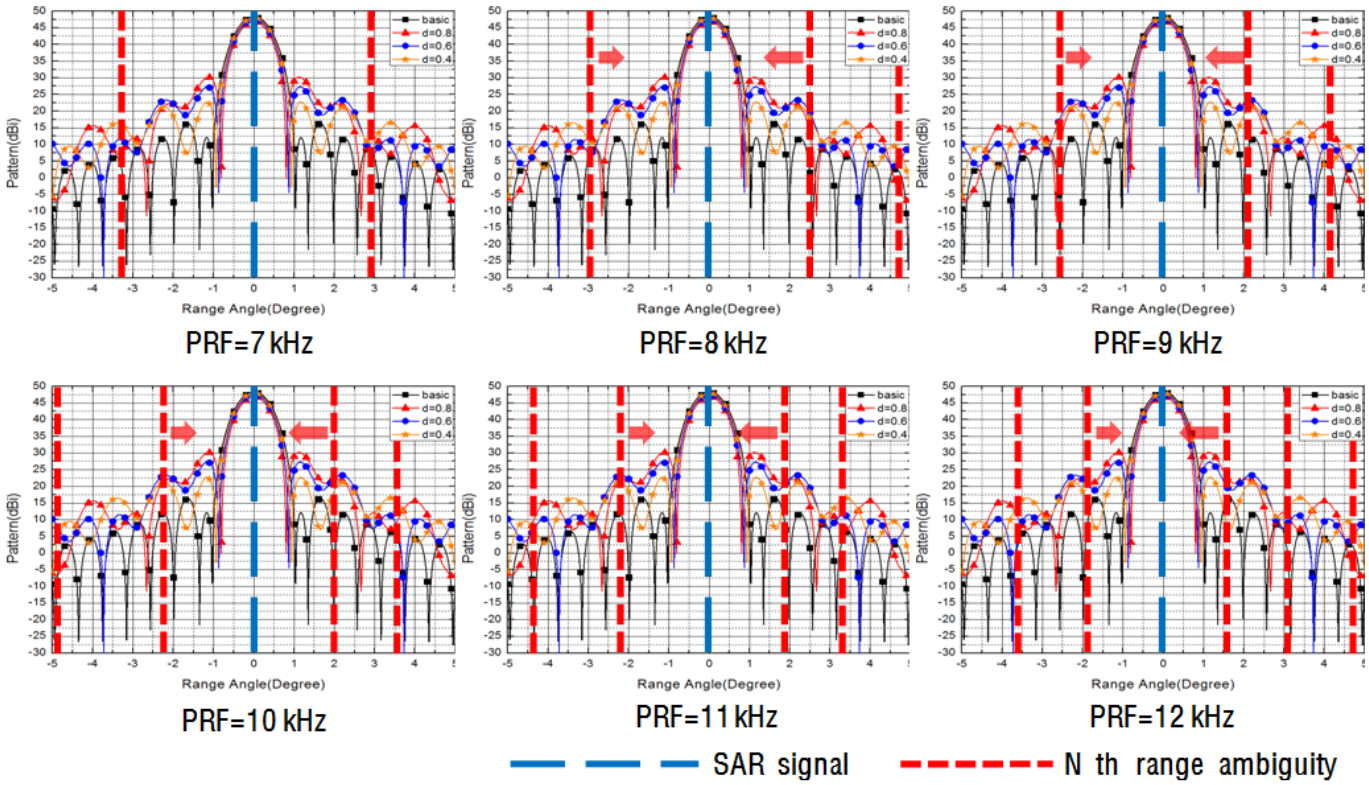

Fig. 7. Rrange ambiguity ratio generating angle in the range direction according to pulse repetition frequency (PRF). SAR = synthetic aperture radar.

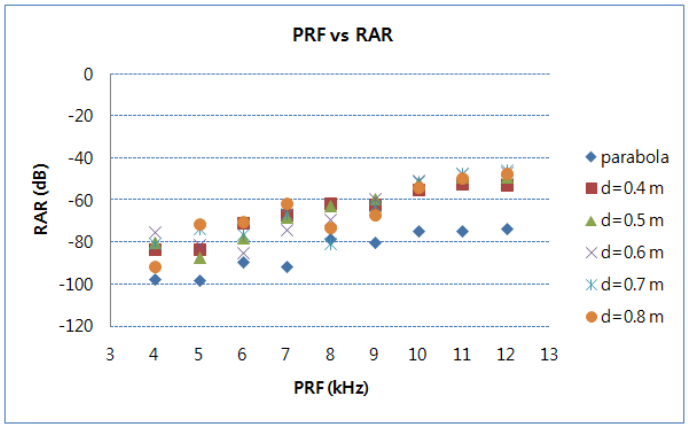

Fig. 8. Range ambiguity ratio (RAR) according to pulse repetition frequency (PRF) and d (the radius of central dish) when the look angle is 30°.

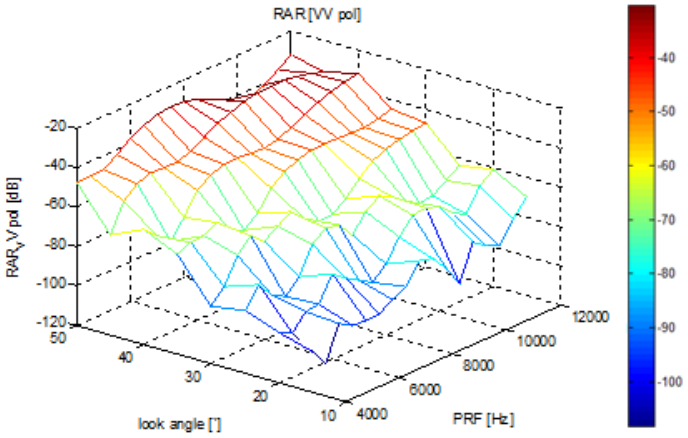

Fig. 9. Range ambiguity ratio (RAR) according to pulse repetition frequency (PRF) and look angle when d is equal to 0.8 m.

to PRF, look angle, and radius of the central dish, d. In general, the RAR increases as the PRF increases. The sidelobe level in the antenna beam pattern due to the size of central dish plays an important role in the RAR evaluation. Fig. 9 shows that increases in the look angle and PRF result in increases in the RAR.

Fig. 10 shows the azimuth ambiguity generating angle according to PRF and processing beamwidth with the radiation pattern of the proposed antenna. The angle generating the azimuthal ambiguity is distant from the main beam angle as the PRF increases whereas in the case of RAR estimation, it was close. On the other hand, it seems that the ambiguity-generating angle, based on the integer n, has a constant interval.

Fig. 11 shows the estimated results of the effects of the central dish on the PRF and AAR. In general, the AAR level is determined by the accumulation of the sidelobe

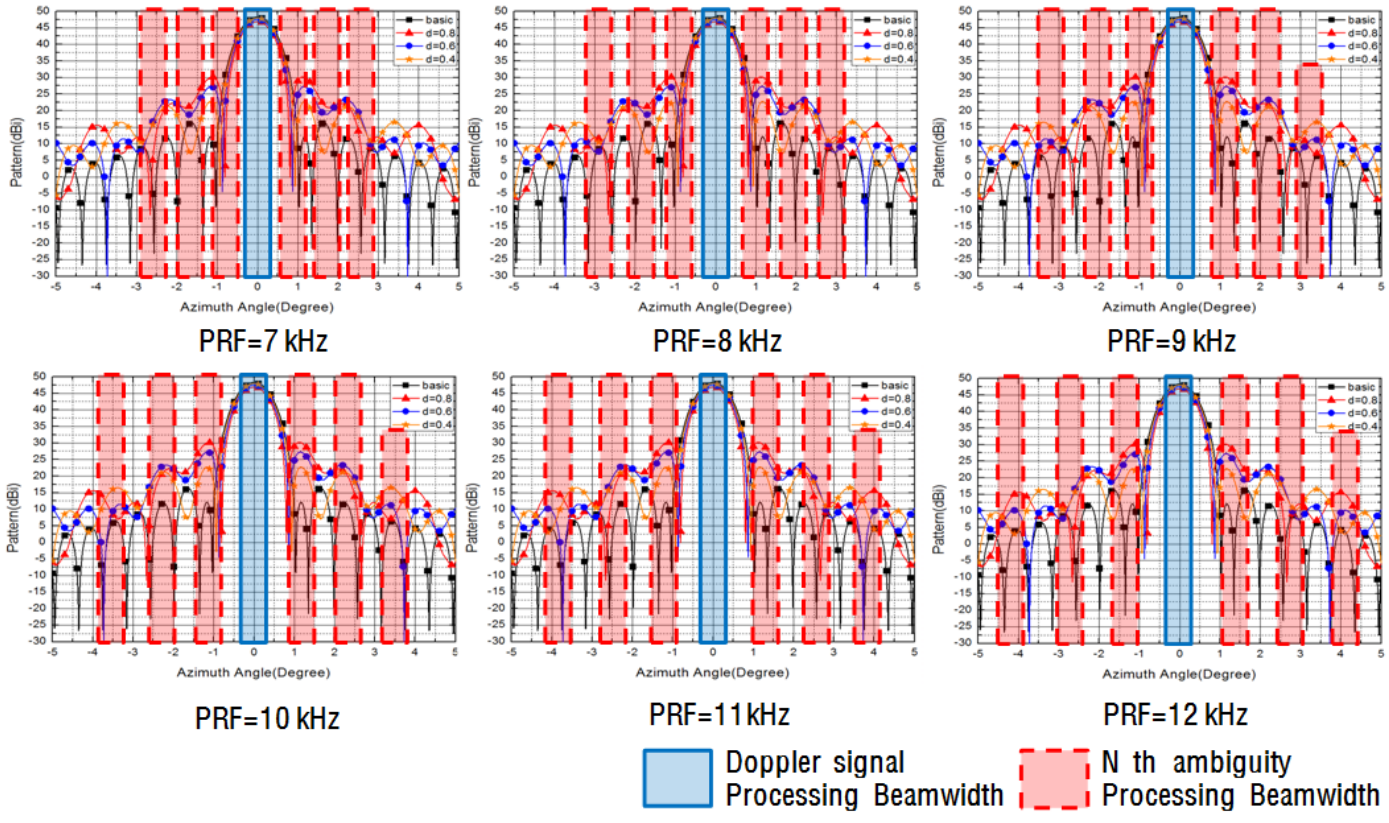

Fig. 10. Azimuth ambiguity generating angle according to pulse repetition frequency (PRF).

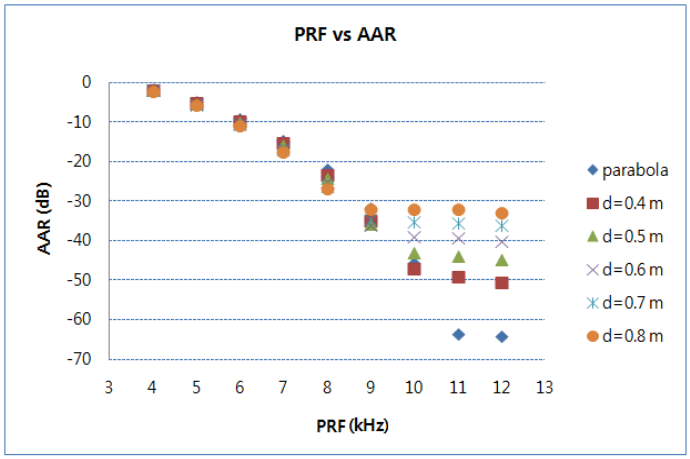

Fig. 11. Azimuth ambiguity ratio (AAR) versus pulse repetition frequency (PRF) according to the variations in d when the look angle is 30°.

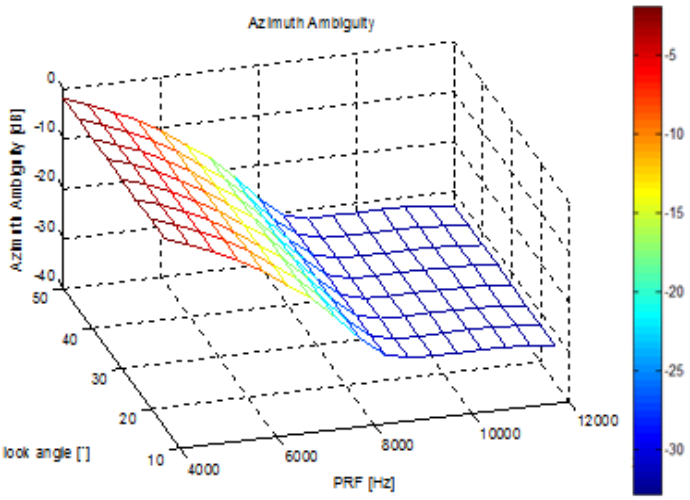

Fig. 12. Azimuth ambiguity ratio (AAR) as a function of pulse repetition frequency (prf) and look angle when d is equal to 0.8 m.

level within the processing beamwidth. The results suggest that a lower AAR level might be predicted as the PRF and the size of d decrease. An important result is that the AAR level is more dependent on the size of the central dish than on the PRF above 10 kHz. Fig. 12 shows the effects of look angle and PRF on the AAR values when the diameter, d of central dish is 0.8 m. In addition, it can be ensured from Fig. 12 that AAR values remain constant independent on look angle.

The estimations of RAR and AAR depending on the PRF, the size of central dish, and the look angle confirm that an appropriate selection of PRF and d (central dish) will lead to an optimum SAR performance. We propose 9 to 10 kHz and 0.6 to 0.8 m as the parameter values for PRF and d, respectively, in order to satisfy the requirement for an AAR level lower than −20 dB.

V. Conclusion

This paper proposed a decision procedure for optimizing the antenna parameters that affect the ambiguity characteristics of SAR performance by carrying out a trade-off on the structure of a parabolic-typed reflector antenna with a central flat dish. The important parameters for SAR performance are RAR and AAR, which have been estimated by calculating the field distributions at the aperture and carrying out full-electromagnetic simulations to obtain the beam pattern according to the variations in antenna parameters. Increasing the radius of the central flat dish was confirmed to increase the sidelobe level and the ambiguity signal level. One advantage of the addition of a central dish to the main reflector antenna is that the total weight will be reduced and the manufacturing process will be simplified. Hence, the selection of the antenna parameters (9 to 10 kHz and 0.6 to 0.8 m as the parameter values for PRF and d, respectively) should be based on this relationship. Our approach will be a good strategy for the system designer when dealing with antenna parameters that affect the ambiguity level.

This work was supported by the Global Surveillance Research Center (GSRC) funded by the Agency for Defense Development.

References

[1] W. A. Imbriale, *Spaceborne Antennas for Planetary Exploration*. New York, NY: John Wiley & Sons, 2006.
[2] A. M. Guarnieri, "Adaptive removal of azimuth ambiguities in SAR images," *IEEE Transactions on Geoscience and Remote Sensing*, vol. 43, no. 3, pp. 625–633, Mar. 2005.
[3] W. Q. Wang, "Mitigating range ambiguities in high-PRF SAR with OFDM waveform diversity," *IEEE Geoscience and Remote Sensing Letters*, vol. 10, no. 1, pp. 101–105, Jan. 2013.
[4] C. Wang, Y. Wang, and M. Liao, "Removal of azimuth ambiguities and detection of a ship using polarimetric airborne C-band SAR images," *International Journal of Remote Sensing*, vol. 33, no. 10, pp. 3197–3210, May 2012.
[5] A. Moreira, "Suppressing the azimuth ambiguities in synthetic aperture radar images," *IEEE Transactions on Geoscience and Remote Sensing*, vol. 31, no. 4, pp. 885–895, Jul. 1993.
[6] B. Grafmuller, A. Herschlein, and C. Fischer, "The TerraSAR-X antenna system," in *Proceedings of the IEEE International Radar Conference*, Arlington, VA, 2005, pp. 222–225.
[7] S. Riendeau and C. Grenier, "RADARSAT-2 antenna," in *Proceedings of the IEEE Aerospace Conference*, Big Sky, MT, 2007, pp. 1–9.

[8] P. Capece, L. Borgarelli, M. Di Lazzaro, U. Di Marcantonio, and A. Torre, "Cosmo Skymed active phased array SAR instrument," in *Proceedings of the IEEE International Radar Conference*, Rome, Italy, 2008, pp. 1−4.
[9] Y. Sharay and U. Naftaly, "TECSAR: design considerations and programme status," *IEE Proceedings Radar, Sonar and Navigation*, vol. 153, no. 2, pp. 117−121, Apr. 2006.
[10] W. L. Stutzman and G. A. Thiele, *Antenna Theory and Design*, 1st ed. New York, NY: John Wiley & Sons, 1981.
[11] M. H. Ka and A. A. Kononov, "Effect of look angle on the accuracy performance of fixed-baseline interferometric SAR," *IEEE Geoscience and Remote Sensing Letters*, vol. 4, no. 1, pp. 65−69, Jan. 2007.
[12] S. Y. Kim, N. H. Myung, and M. J. Kang, "Antenna mask design for SAR performance optimization," *IEEE Geoscience and Remote Sensing Letters*, vol. 6, no. 3, pp. 443−447, Jul. 2009.

Seong Sik Yoon

received the B.S. and M.S. degree in electronics, telecommunications, and computer engineering from Korea Aerospace University, Goyang, Korea, in 2010 and 2013, respectively. He is currently working toward the Ph.D. degree at the Microwave and Millimeterwave Solution Lab of Korea Aerospace University. His research interests include satellite communication antenna, radar antenna design and analysis. His current interests are multipactor in waveguide and measurement of composite material.

Taek Kyung Lee

received the B.S. degree in electronic engineering from Korea University, Seoul, Korea, in 1983, and the M.S. and Ph.D. degrees in electrical engineering from the Korea Advanced Institute of Science and Technology, Seoul, in 1985 and 1990, respectively. From May 1990 to April 1991, he was a Postdoctoral Fellow with the University of Texas at Austin (under a grant from the Korea Science and Engineering Foundation). From August 1991 to February 1992, he was with the Korea Advanced Institute of Science and Technology. In March 1992, he joined the faculty of Korea Aerospace University, Goyang, Korea, where he is currently a Professor with the School of Electronics, Telecommunication, and Computer Engineering. From July 2001 to July 2002, he was an Associate Visiting Research Professor with the University of Illinois at Urbana-Champaign. His research interests include computational electromagnetics, antennas, analysis and design of microwave passive circuits, and geophysical scattering.

Jae Wook Lee

received the B.S. degree in electronic engineering from Hanyang University, Seoul, Korea, and the M.S. and Ph.D. degrees in electrical engineering (with an emphasis in electromagnetics) from Korea Advanced Institute of Science and Technology (KAIST), Daejeon, Korea, in 1992, 1994, and 1998, respectively. From 1998 to 2004, he was a senior member in the Advanced Radio Technology Department, Radio and Broadcasting Research Laboratory, Electronics and Telecommunications Research Institute (ETRI), Daejeon. He later joined the School of Electronics, Telecommunications and Computer Engineering, Korea Aerospace University, Korea, where he is currently a Professor. His research interests include high power amplifier design, computational electromagnetics, EMI/EMC analysis on PCB, and component design in microwave and millimeterwave.

Dong Woo Yi

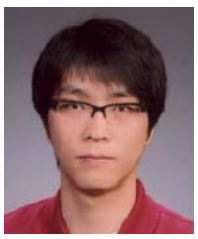

received the B.S. degree in electronics, electric wave engineering from Chungnam University, Daejeon, Korea, and M.S. degrees in electrical engineering from Pohang University of Science and Technology in 2003, 2005, respectively. He is currently working at Agency for Defense Development. His research interests include image radar antenna design.